Properties of Deflagration Fronts and Models for Type Ia Supernovae

I. Domínguez [1], P. Höflich[2]

[1] *Dept. de Física de Teórica y del Cosmos, Universidad de Granada, Granada, Spain*

[2] *Dept. of Astronomy, University of Texas, Austin, TX 78712 USA*

ABSTRACT

Detailed models of the explosion of a white dwarf, which include self-consistent calculations of the light curve and spectra, proved a link between observational quantities and the underlying explosion model. These calculations assume spherical geometry and are based on parameterized descriptions of the burning front. Recently, first multi-dimensional calculations for nuclear burning fronts have been performed. Although a fully consistent treatment of the burning fronts is beyond the current state of the art, these calculations provided a new and better understanding of the physics. Several new descriptions for the flame propagation have been proposed by Khokhlov et al. and Niemeyer et al.. Using various description for the propagation of a nuclear deflagration front, we have studied the influence on the results of previous analyses of Type Ia Supernovae, namely, the nucleosynthesis and structure of the expanding envelope.

Our calculations are based on a set of delayed detonation models with parameters that give a good account of the optical and infrared light curves, and of the spectral evolution. In this scenario, the burning front propagates first in a deflagration mode and, subsequently, turns into a detonation. The explosions and light curves are calculated using a one-dimensional Lagrangian radiation-hydro code, including a detailed nuclear network.

We find that the results of the explosion are rather insensitive to details of the description of the deflagration front, even if its speed and the time till the transition to detonation differ by almost a factor of two. For a given white dwarf (WD) and a fixed transition density, the total production of elements changes by less than 10 %, and the distribution in the velocity space changes by less than 7 %. Qualitatively, this insensitivity of the final outcome of the explosion on the details of the flame propagation during the (slow) deflagration phase can be understood as follows: For plausible variations in the speed of the turbulent deflagration, the duration of this phase is several times longer than the sound crossing time in the initial WD. Therefore, the energy produced during the early nuclear burning can be redistributed over the entire WD causing a slow pre-expansion. In this intermediate state the WD is still bound but its binding energy is reduced by the amount of nuclear energy. The expansion ratio depends mainly on the total amount of burning during the deflagration phase. Consequently, the conditions are very similar under which nuclear burning takes place during the subsequent detonation phase. In our example, the density and temperature at the the burning front changes by less than 3 % , and the expansion velocity changes by less than 10 % . The burning

conditions are very close to previous calculations which used a constant deflagration velocity. Based on a comparison with observations, those required low deflagration speeds ($\approx$ 2 to 3 % of the speed of sound). An exception to the similarity are the innermost layers of $\approx$ 0.03 to 0.05 $M_\odot$. Still, nuclear burning is in nuclear statistical equilibrium (NSE) but the rate of electron capture is larger for the new descriptions for the flame propagation. Consequently, the production of very neutron rich isotopes is increased. In our example and close to the center, Y_e is about 0.44 compared to 0.46 in the model with constant deflagration speed. This increases the ^{48}Ca production by more than a factor of 100 to $3.E-6 M_\odot$.

Conclusions from previous analyses of light curves and spectra on the properties of the WD and the explosions will not change and, even with the new descriptions, the delayed detonation scenario is consistent with the observations. Namely, the central density, results with respect to the chemical structure of the progenitor and the transition density from deflagration to detonation do not change. The reason for this similarity is the fact that the total amount of burning during the long deflagration phase determines the restructuring of the WD prior to the detonation. Therefore, we do not expect that the precise, microphysical prescription for the speed of a subsonic burning front has a significant effect on the outcome.

However, on the current level of uncertainties for the burning front, the relation between properties of the burning front and of the initial white dwarf cannot be obtained from a comparison between observation and theoretical predictions by 1-D models. Multidimensional calculations are needed to get an inside into the relations between model parameters such as central density and properties of the deflagration front, its relation to the transition density between deflagration and detonation, and to make use of information on asphericity that is provided by polarization measurements.

These questions are essential to test, estimate and predict some of the evolutionary effects of SNe Ia and their use as cosmological yard stick.

Subject headings: Supernovae: general, – nucleosynthesis, abundances – turbulence

1. Introduction

The standard scenario for Type Ia Supernovae consists of massive carbon-oxygen white dwarfs (WDs) with a mass close to the Chandrasekhar mass which accrete through Roche-lobe overflow from an evolved companion star (Whelan & Iben 1973; Nomoto & Sugimoto 1977). In these accretion models, the explosion is triggered by compressional heating. From the theoretical standpoint, the key questions are how the flame ignites and propagates through the white dwarf. Several models within this general scenario have been proposed in the past including detonations, deflagrations and the delayed detonations, which assume that the flame starts as a deflagration and turns into a detonation later on (Khokhlov 1991, Yamaoka et al. 1992, Woosley & Weaver 1994). The latter scenario and its variation "pulsating delayed detonation", seems to be the most promising one, because, from the general properties and the individual light curves and spectra, it can account for the majority of SNe Ia events (e.g. Höflich & Khokhlov 1996, and references therein). We note that with the discovery of the supersoft X-ray sources, potential progenitors have been found (e.g. van den Heuvel et al. 1992; Rappaport et al. 1994).

What we observe as a supernova event is not the explosion itself but the light emitted from a rapidly expanding envelope produced by the stellar explosion. As the photosphere recedes, deeper layers of the ejecta become visible. A detailed analysis of the light curves and spectra gives us the opportunity to determine the density, velocity and composition structure of the ejecta and provide a direct link to observations. A successful application of observational constrains requires both accurate early light curves (LC) and spectral observations and detailed theoretical models which are coupled tightly to the hydrodynamical calculations (e.g. Harkness 1991, Höflich, Khokhlov & Müller 1991, Bravo et al. 1996). According to previous results, normal bright SNe Ia can be explained by delayed detonation and pulsating delayed detonation models (e.g. SN 94D, Höflich 1995). During the deflagration phase, the deflagration velocity is 3 % of the sound speed. In general, a transition from deflagration to detonation is required at densities of about $2 - 2.5\ 10^7\ g\ cm^{-3}$. Central densities of the initial WDs are $\approx 2.0\ 10^9 g\ cm^{-3}$. Despite their success, the hydrodynamical models are limited by the parametrized description of the burning front and the ad hoc adjustment of the density at which the deflagration turns into a detonation.

Recently, significant progress has been made toward a better understanding of the propagation of nuclear burning fronts. First multidimensional hydrodynamic calculations of the deflagration fronts have been performed (e.g. Khokhlov 1995, Niemeyer & Hillebrandt 1995). A basic, qualitative understanding of the mechanism which leads to a transition from a deflagration to a detonation phase may have been achieved (Khokhlov, Oran & Wheeler 1997ab, Niemeyer & Woosley 1997). Qualitatively, the results agree between different hydrodynamical numerical simulations but a full description of the deflagration in the entire white dwarf and the consistent calculations of the transition requires high resolution in 3-D that are beyond the current state of the art. Note that the cited references rely on their subgrid models and did not resolve the turbulent deflagrations on small scales and for appropriate Reynolds numbers. Moreover, the transition from a deflagration to a detonation is still not well understood.

Here, the question is addressed how our results of the explosions vary if we use descriptions for the deflagration front which use functional relations derived from 3-D calculations.

1.1. Hydrodynamics

The explosions are calculated using a one-dimensional radiation-hydro code, including nuclear networks (Höflich & Khokhlov 1996, and references therein). This code solves the hydrodynamical equations explicitly by the piecewise parabolic method (Collela & Woodward 1984) on ≈ 1000 radial zones. The zones near the burning front are subdivided to properly track its propagation. The code includes the solution of the frequency-averaged radiation transport implicitly via moment equations, expansion opacities, and a detailed equation of state. The frequency-averaged variable Eddington factors and mean opacities are calculated by solving the frequency-dependent transport equations. About one thousand frequencies (in one hundred frequency groups) and about five hundred depth points are used. Nuclear burning is taken into account using a network of 218 nuclei (see Thielemann, Nomoto & Hashimoto 1996, Höflich, Wheeler & Thielemann 1998, and references therein).

1.2. Description of the Burning Front

We have considered three cases:

Case 1) $v_{burn} = const.\ v_{sound}$. In our previous investigations, const=0.03 has been found to give the best fits to observations. This corresponds to the fractal dimension D= 2 in the description of Woosley & Weaver (1994) which suggested $D = 2$ to 2.5.

Case 2 & 3) Here we assumed that $v_{burn} = max(v_t, v_l)$ where v_l and v_t are the laminar and turbulent velocities, respectively. v_l is calculated according Khokhlov et al. (1997a).

Intrinsically, turbulent combustion is a three- dimensional problem. It is driven on large scales by the buoyancy of the burning products. The turbulent cascade penetrates down to very small scales, and makes the rate of deflagration independent of the microphysics. Turbulent combustion in a uniform gravitational field and static conditions singles out the propagation of the flame against gravity g. Chemical combustion experiments have been performed in confined environments, so called Cumbustion chambers. These experiments can be reproduced by numerical simulations. The propagation speed can be described by

$$v_t = C_1\ \sqrt{\alpha_T\ g\ L_f};\quad C_1 = 0.5;$$
$$\alpha_T = (\alpha - 1)/(\alpha + 1),\ \alpha = \rho^+(r_{burn})/\rho^-(r_{burn}) \qquad Eq.[1]$$

where α_T is the Atwood number, L_f is the characteristic length scale, and ρ^+ and ρ^- are the densities in front and behind the front, respectively. However, despite the success in terrestrial experiments, the basic assumptions of both a uniform gravitational field and static conditions are violated in the rapidly expanding envelopes of SNe Ia. The main effect of expansion is the freeze out of the turbulence on scales L_f where the turbulent velocity due to Rayleigh Taylor instabilities is comparable to the differential expansion velocities on those scales, i.e.

$$v_t \approx v_{exp} = L_f/\tau_{ex} \qquad Eq.[2]$$

Based on this idea, Khokhlov et al. (1997b) suggested to use the average turbulent velocity (eq. 1), use α for uniform, static conditions, and to use the mean expansion time scale determined by one dimensional simulations $\tau_{exp} \approx dt/d\ ln\ R_{WD}$. He found for the propagation speed of the turbulent burning front

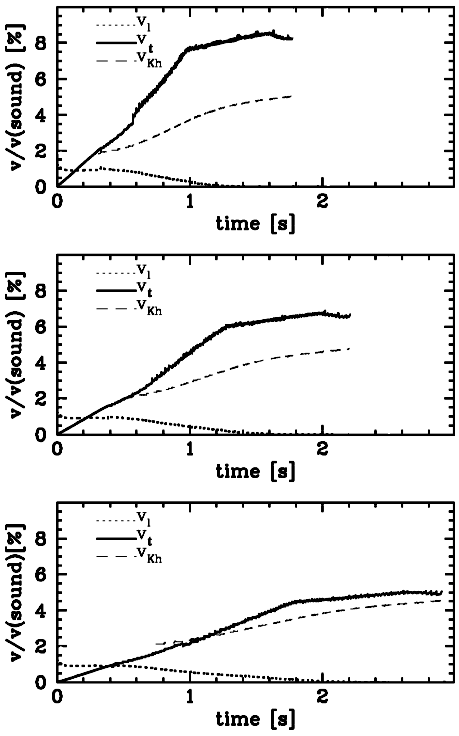

Fig. 1.— Laminar and turbulent velocities at the burning front for models according eq. 1 with C_1= 0.25, 0.20 and 0.15 (top to bottom, m2z02y24i3...1). For comparison, v_{Kh} gives the velocity of the burning front according to Khokhlov (eq. 2, m2z02y24i4).

$$v_t = 0.0474 * \sqrt{(g\ L_f)} \qquad Eq.[3]$$

As third case for the description, we followed the recipe of Khokhlov but did some modifications by taking α, L_f and τ_{exp} directly from the hydro at the location of the burning front. Freeze-out was assumed when the radius of a mass element has doubled after being burned. C_1 in equation [1] has been varied. Note that a variation in C_1 is equivalent to scaling the relative length scale for the freeze out. We varied C_1 in the range to cover a parameter space which includes both the descriptions suggested by Khokhlov et al. (1997b) and Niemeyer & Woosley (1997).

2. Results

The influence of the description of the deflagration front has been studied at the example of a set of delayed detonation model based on the same C/O

WD with a mass of 1.39 $M_\odot$ and a central density $\rho_c = 2.0\ 10^9 g\ cm^{-3}$. In all cases, a transition density ρ_{tr} of $2.3\ 10^7 g\ cm^{-3}$ has been assumed. The description of the deflagration front has been varied. The deflagration velocity is taken to be 3 % of the speed of sound v_{sound} for *m2z02y24i5*, and the approximation of Khokhlov is used for *m2z02y24i4*. Eq. (1) has been used for models *m2z02y24i1-3* with C_1=0.15, 0.20 and 0.25. M2 indicates that the initial mass of the progenitor was 2 $M_\odot$, with solar metallicity (z02), and 24 % of Helium.

In figure 1, the velocity of the burning front is shown as a function of time. In general, the speed of the burning front is mainly determined by the turbulent speed but the very early time. As can be expected, the transition density is reached later in time for smaller v_t because the lower energy production per time and, consequently, the slower pre-expansion.

The final density, velocity and chemical structures for the most important elements are given in Figs. 2 and 3. Overall, the structures are very similar because the total energy release depends on the amount of the released energy and the initial structure of the WD. Even the chemical structure or, more precisely, the location of transition between different regimes of burning (e.g. from partial to total Si-burning) varies between all models by ≤ 7 % in the space of the final expansion velocity. The total production of the most abundant elements changes by only 4 % and 3 % with mean values of 0.60 and 0.16 $M_\odot$ for $M(^{56}Ni)$ and $M(Si)$, respectively.

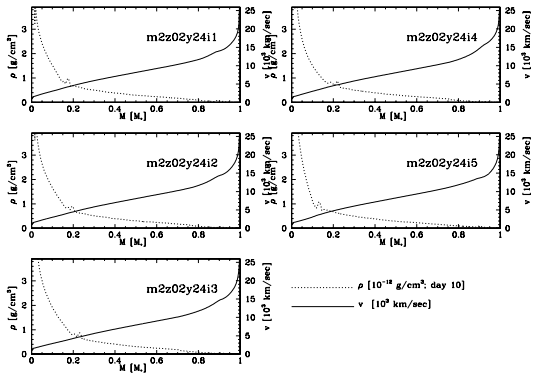

Fig. 2.— Final density and velocity as a function of mass for different models (see text).

At first, one may expect a rather high sensitivity of the final burning products on details of the description of the burning front (Hillebrandt, Niemeyer & Woosley 1997) but the tests show a low insensitivity (Fig.2 ... 3). This result can be understood by the very nature of delayed detonation models. Qualitatively, the low dependence on the details of the flame propagation during the (slow) deflagration phase can be understood as follows: The production of intermediate mass elements depends on the expansion of the outer envelope before the burning front 'arrives'. This pre-expansion occurs during the deflagration phase. For plausible variations in the speed of the turbulent deflagration, the duration of this phase is several times longer than the sound crossing time in the initial WD. Therefore, the energy produced during the early nuclear burning can be redistributed over the entire WD causing a smooth lifting/preexpansion. In this intermediate state the WD is still bound but its binding energy is reduced by the amount of nuclear energy. The expansion ratio depends mainly on the total amount of burning during the deflagration phase. Consequently, the conditions are very similar

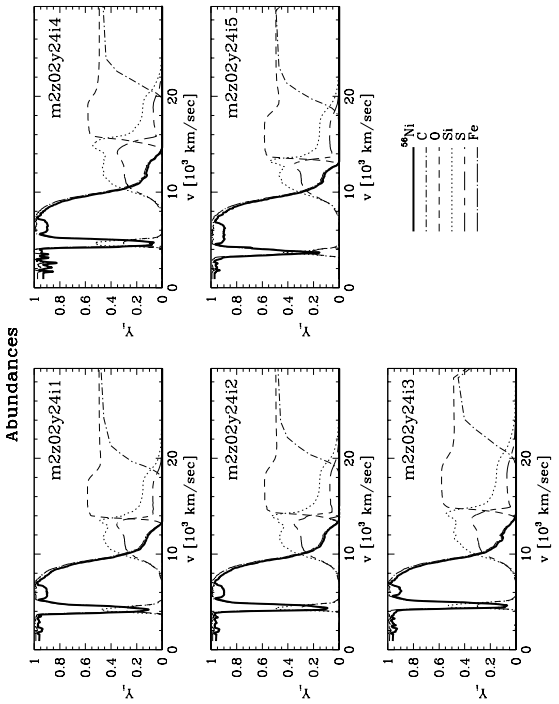

Fig. 3.— Same as Fig.2 but final chemical composition as a function of mass.

under which nuclear burning takes place during the subsequent detonation phase. In Fig. 4, the burning conditions just behind the front are given for the two extreme models with $C_1 = 0.15$ and $C_1 = 0.25$. The durations of the deflagration phase are about 1.7 and 2.9 seconds, respectively.

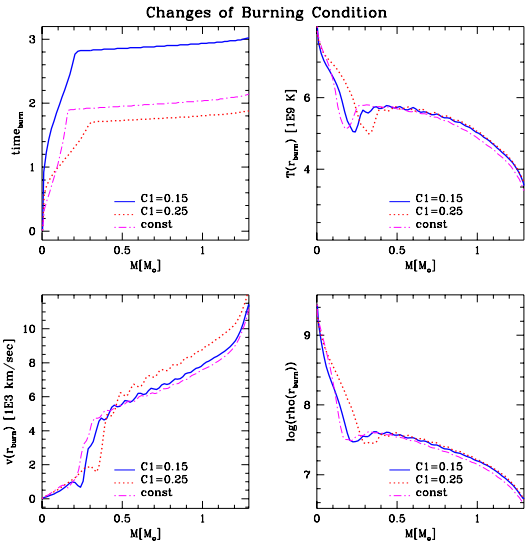

Fig. 4.— Time at which a mass element is burned, mean expansion velocity, density and temperature behind the burning front for deflagration speeds with variable speed according eq. 1 with with various C_1 (m2z02y24i3/1) and with constant deflagration speed (m2z02y24i5). We use arithmetic means over 0.05 $M_\odot$.

Both models start with laminar deflagrations, i.e. the conditions under with nuclear burning takes place are similar. After about 3 % of a solar mass has been burned, the flame speed is determined by the turbulent speeds which differ by about 70 %, and the densities behind the burning front differ significantly. However, in all models, the temperatures are sufficient high to burn up to NSE and, mainly, ^{56}Ni is produced. After burning of about 0.25 and 0.32 $M_\odot$ for the models with low and high turbulent speeds, the transition between the burning as a deflagration to a detonation is triggered. Outside $\approx 0.4 M_\odot$, the densities and consequently the temperatures are very similar. Note that the layers of partial burning are located above $\approx 0.6 M_\odot$. The expansion rate, relevant for the time scale for adiabatic cooling, differ by 7 % only. This similarity in the burning conditions explains the insensitivity in the final chemical profiles. The pre-expansion is even more similar than can be expected from this argument because the hydrodynamical time scales for energy redistribution is $\approx$ 1 second. Thus, the influence of the burning in the deflagration mode during the few tenth of a second before turning to a detonation is reduced with respect to the pre-expansion of the outer layers. As soon as the front turns into a detonation, the remainder of the WD is burned almost 'instantly' or, better, on nuclear time scales.

For comparison, the properties at the burning front are given for the description with $v_{burn}/v_{sound} = const. = 0.03$ where the constant has been tuned to give good agreement between the observed and calculated light curves and spectra (e.g Höflich & Khokhlov 1996). This description for the burning front is widely used in literature and it is consistent with constrains from the nucleosynthesis (e.g. Brachwitz et al. 1998, Khokhlov 1991, Thielemann et al. 1997, Woosley & Weaver 1994 with D=2).

In the outer layers, the burning conditions are virtually identical to $C_1 = 0.15$ including the expansion rate. Slightly less material is burned during the deflagration phase because the front is faster and the initial energy production is larger during the first second (Fig. 1.).

Note that the amount of burning under very high densities and, therefore, the production of neutron rich isotopes in the central region of the WD depends sensitively on the speed of the front which, in the more realistic descriptions starts with laminar speed. In comparison with previous calculations, this boosts the production of very neutron rich isotopes such as ^{48}Ca. In our example and close to the center, Y_e is about 0.44 compared to 0.46 in the model with constant deflagration speed. This increases the ^{48}Ca production from $2\times10-8 M_\odot$ to $3\times10^{-6} M_\odot$. This increase is the same for all models which start with the laminar deflagration speed. For a systematic study of different flame speeds, see the PhD thesis of Brachwitz (1999). Note that the production of neutron rich isotopes depend on the central density and whether the ignition is very close to the center or off-center. In principle, this opens a new window for detailed analyses of the progenitor and the ignition process in SNe Ia.

3. Conclusions

The final structure of the expanding envelope is rather insensitive to the detailed description of the burning front during the deflagration phase. It depends mainly on global quantities, namely the total amount of burning during the deflagration phase and the sound speed in the initial white dwarf. Therefore, the detailed, spatial structure of the burning front cannot be expected to change the result of the explosion. Findings from previous analyses of light curves and spectra on the properties of the WD and the explosions will not change and(!) the new description of the deflagration front is consistent with the observations. The central density, conclusions about the chemical structure of the progenitor and the transition density from deflagration to detonation do not change. Differentially, evolutionary effects and its consequences for the observations can be explored by parameterized models.

The validity of the transition density found in previous analysis also poses a question on our understanding of the transition from turbulent deflagration to detonation which is not well understood. Currently, it is attributed to the Zeldovich mechanism which is based on the adiabatic mixing of burned and unburned material where the entropy increase in the unburned fuel triggers the explosion (Khokhlov et al. 1997b, Niemeyer et al. 1997). The relative change over the entire range of parameterizations discussed here corresponds to a change in the transition density of $\approx 10\%$. This leaves us with the puzzle why the theoretical estimates for the transition density are lower by a factor of about 0.7 (Khokhlov et al. 1997b) and 0.4 (Niemeyer et al. 1997). For reasons, we can only speculate. The differences between the latter values may indicate the size of the uncertainties in our understanding of this transition process. Other, not yet considered microscopic effects may be involved. Another possibility may be that we measure two different things. To derive the model parameters from the observations, we measure the mean density at the burning front when the transition occurs whereas the theoretical considerations provide information on the location where the transition occurs. Maybe the fragmentation of the burning front causes that the transition occurs somewhat ahead of the mean front. If this interpretation is correct, this may indicate that the detonation is started at about 10 to 20 % (in radius) ahead of the mean front. In either case, a clarification needs further investigations and, certainly, will provide new inside into the properties of nuclear burning fronts.

We note that the nucleosynthesis, optical and IR spectra and light curve seem to require that, after an initial phase of slow burning, the front moves with velocities close to the speed of sound to keep up with the expanding outer layers and to burn Carbon under low density conditions. The latter is indicated by a strong line at 1.05 μm which can be attributed to Mg II and indicates expansion velocities in excess 15,000 ... 16,000 km/sec. In general, unburned Carbon is restricted to velocities above 20,000 km/sec (Fisher et al. 1997, Höflich 1995, Höflich & Khokhlov 1996, Khokhlov 1991, Nugent et al. 1997, Thielemann et al. 1996, Wheeler et al. 1998). Both the high velocities in Mg and C are consistent with delayed detonation models but inconsistent with the classical deflagration model W7 (Nomoto et al. 1984). Extended mixing of the inner, Ni-rich layers can be excluded from the spectra (Höflich, Wheeler & Thielemann 1998). Mixing of the outer layers may produce Si lines at high velocity (Nugent et al. 1997) but does not solve the problems with Mg and C. Although the evidence favors the delayed detonation scenario in the framework of 1-D models, this does not necessarily imply that a transition from detonation occurs. Alternatively, the flame may propagate as a very fast deflagration wave (Hillebrandt, private communication). In this context, the transition density may be attributed to the region where the turbulent flame is not any more driven by Rayleigh-Taylor instabilities.

Finally, we have also to stress the limits of 1-D models with a parameterized description of the deflagration front and the need for multidimensional hydrodynamical calculations and radiation transport. These limits are critical to understand details of the explosion and to use SNe Ia as distance indicators on cosmological scales (e.g. Schmidt et al. 1998, Perlmutter et al. 1999). Observations clearly showed a strong relation between the maximum brightness and the decline relation (Phillips 1993). From theoretical models, the amount of radioactive nickel produced during the explosion of a massive white dwarf has been identified as the basic quantity which provides this relation. The relation is independent from details of the model, however, the amount of ^{56}Ni actually produced depends on a combination of free parameters in the models such as central density and the chemical composition of the WD, and the propaga-

tion of the burning front. If these parameters are varied independently within the limits indicated by individual fits to observations (Höflich & Khokhlov 1996), we expect a spread around the mean maximum brightness/decline relation of $\approx 0.4^m$ which is consistent with the spread based on the CTIO data published by Hamuy et al. (1996). Recent redefinitions of the statistical methods and new observations suggest a much tighter relation with a spread of $\approx 0.12^m$ (Schmidt et. al. 1998). This narrow spread cannot be understood in the context of the parameter range allowed by current analyses. This tight relation may hint of an underlying coupling of the progenitor, the accretion rates and the propagation of the burning front. However, on the current level of uncertainties, the relation between the free parameters such as transition density and initial central density cannot be deduced from a comparison between observation and theoretical predictions by 1-D models. Multidimensional calculations are needed to test e.g. the relation between chemical composition or central density of the white dwarf and the properties of the deflagration front and its relation to the transition density between deflagration and detonation.

In general, the chemical signature of the deflagration phase is 'wiped out' by the detonation front but a small trace may remain at the interfaces between complete and incomplete Si burning (Thielemann et al. 1996). Although not conclusive, recent polarization measurement may already hint toward the existence of such inhomogeneities in the chemical structure (Wang, Wheeler & Höflich 1998).

ACKNOWLEDGMENTS

We would like to thank our colleagues A. Khokhlov, J. Niemeyer and C. Wheeler for helpful discussions and comments. I. Domínguez would like to thank C. Wheeler and his colleagues for the hospitality during her stay in Austin where this work was started. P. Höflich would like to thank Prof. E. Battaner and his colleagues for the hospitality during his visit at the University of Granada where this work was finished. This research was supported in part by NASA Grant LSTA-98-022, and the PB96-1428 of the Ministery of Education in Spain. The calculations were done on a cluster of workstations financed by the John W. Cox-Fund of the Department of Astronomy at the University of Texas and the High-Performance-Center at the University of Texas at Austin.

REFERENCES

Bravo E., Tornambe A., Domínguez I. Isern J. 1996, AA, 306, 811

Brachwitz, F.; Iwamoto, K.; Thielemann, F.-K.; Nomoto, K., 2nd Oak Ridge Symposium, ed. A. Mezzacappa, Inst. of Physics Publishing, 1998, 681

Brachwitz F. 1999, PhD-thesis at the University of Basel, supervised by F.K.Thielemann, Switzerland

Collela P., Woodward P.R. 1984, J.Comp.Phys., 54, 174

Fisher A., Branch D., Nugent P., Baron E. 1997, ApJ, 481L, 89

Hamuy M., Phillips M.M, Maza J., Suntzeff N.B., Schommer R.A, Aviles A. 1996, AJ, 112, 2438

Harkness, R.P. 1991, in: SN1987A, ed. I.J. Danziger, ESO, Garching, p.447

Hillebrandt W., Niemeyer J., Woosley S. 1997, in: Thermonuclear Supernovae, eds. Canal et al., Kluwer Academic Publisher, Vol. 486, 337

Höflich, P., Khokhlov, A., Müller, E. 1991, A&A, 248, L7

Höflich, P. 1995, ApJ, 443, 533

Höflich P., Khokhlov A. 1996, ApJ, 457, 500

Höflich P., Wheeler J.C., Thielemann F.K. 1998, ApJ, 495, 617

Khokhlov A. 1991, A&A, 245, 114

Khokhlov A. 1995, ApJ, 449, 695

Khokhlov A., Oran E.S., Wheeler J.C. 1997a, ApJ, 478, 678

Khokhlov A., Oran E.S., Wheeler J.C. 1997b, in: Thermonuclear Supernovae, eds. Canal et al., Kluwer Academic Publisher, Vol. 486, 475

Niemeyer J.C., Hillebrandt W. 1995, ApJ, 452, 779

Niemeyer J.C., Woosley S. 1997, ApJ, 475, 740

Nomoto K., Sugimoto D. 1977, PASJ, 29, 765

Nugent P., Baron E., Branch D., Fisher A., Hausschild P. 1997, ApJ, 485, 812

Perlmutter S. et al. 1999, ApJ, in press

Phillips M. M., 1993, ApJ, 413, L108

Rappaport S., Chiang E., Kallman T., Malina R. 1994 , ApJ, 431, 237

Schmidt M. et al. 1998, ApJ, 507, 46

Thielemann F.K., Nomoto K., Hashimoto M. 1996, ApJ, 460, 408

Thielemann F.K, Nomoto K., Iwamoto K., Brachwitz F., in: Thermonuclear Supernovae, eds. Ruiz-Lapuente et al., NATO ASI-Series, Series C, Vol. 486, p. 485

Wang L., Wheeler J.C., Höflich P. 1998, ApJ, 476, 27L

Wheeler J.C., Höflich P., Harkness R., Spyromillio J., 1998, ApJ, 496L, 908

Whelan J., Iben I. Jr. 1973, ApJ, 186, 1002

Woosley S. E., Weaver T. A. 1994, in: Supernovae, Elsevier, Amsterdam, 423

Van den Heuvel E.P.J., Bhattacharya D., Nomoto K., Rappaport S. 1992, A&A, 262, 97

Yamaoka H., Nomoto K., Shigeyama T., Thielemann F. 1992, A&A, 393, 55

This 2-column preprint was prepared with the AAS LaTeX macros v4.0.